Downscaled extremes based on NCEP reanalysis data (1958–2000): Primary Region — Alps

Jürg Schmidli

ETH partner report for deliverable D12 — December 3, 2003

Introduction

The purpose of deliverable D12 is to compare different downscaling methods based on the NCEP reanalysis. This partner report describes the results for precipitation of the local rescaling method for ten stations in the Alpine region from the FIC station data set.

Method

As our main predictor we use GCM simulated precipitation, and as a secondary predictor the $1000\ \mathrm{hPa}$ geopotential height field. Four statistical downscaling methods are investiaged: (i) local rescaling of GCM simulated precipitation (LOC), (ii) local rescaling with bias correction for precipitation frequency and intensity (LOCI), (iii) local rescaling with a dynamical correction (DYN), and (iv) local rescaling with a dynamical correction and bias correction for precipitation frequency and intensity (DYNI) (see also Widmann and Bretherton, 2003). The intended application for these four methods is to downscale from the GCM scale to the regional scale in order to produce mesoscale gridded precipitation fields. However, for the purpose of this intercomparison, the methods are applied directly to station data. The first two methods use GCM simulated precipitation as their only predictor. The third and fourth method require in addition to the GCM simulated precipitation a proxy of the large-scale flow. Here the first three principal components of the geopotential height field at $1000\ \mathrm{hPa}$ is used. While the first two methods are calibrated on a monthly basis, the latter two methods are calibrated seasonally. The two latter methods can be regarded as a flow-dependent bias correction of GCM precipitation.

Local Rescaling

The downscaled precipitation $\hat{P}$ for a given station can be written as

$$\hat{P}(t) = s(\tau)P^m(t)$$

where P^m is the (GCM) model precipitation, τ represents the month of the year and

$$s(\tau) = \frac{\mu(P \geq P_0, \tau)}{\mu^m(P^m \geq P_0^m, \tau)}$$

is a scaling factor. The scaling factor for LOC (LOCI) is equal to the fraction of the unconditional (conditional) mean of observed versus model precipitation. For LOCI, the wet-day cutoff for the observations is $P_0 = 1\ \mathrm{mm}$. The wet-day cutoff for the model precipitation P_0^m is determined such that the model precipitation frequency equals the observed precipitation frequency.

Dynamical Rescaling

The downscaled precipitation $\hat{P}$ for a given station can be written as

$$\hat{P}(t) = s(\tau, Z_k^m)P^m(t)$$

where the scaling factor s now depends on the large-scale circulation, and τ represents the season of the year. For details of the basic method see Widmann and Bretherton (2003)

Data

This evaluation is based on ten stations in the Alpine region from the FIC station data set, and NCEP data interpolated onto HadAM grid points (see Fig. 1). For each station the grid point with the highest correlation with the corresponding daily station data is selected (see Table. 1).

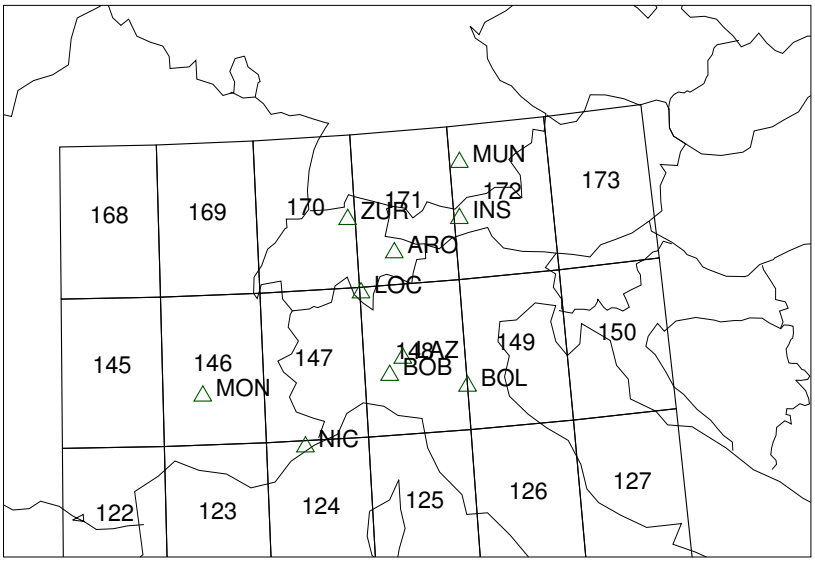

Figure 1: The 18 HadAM grid points and the 10 Alpine stations from the FIC station data set (see Table 1).

Table 1: The ten stations in the Alpine region from the FIC station data set. The column GP indicates the HADAM grid point used for downscaling.

Station	lon	lat	height	GP
Innsbruck	11.38	47.25	578	172
Montelimar	4.73	44.58	74	146
Nice	7.20	43.65	10	123
München	11.50	48.16	515	172
Bologna	11.25	44.48	60	126
Lazzaro Albernoi	9.71	45.03	50	149
Bobbio	9.36	44.76	270	125
Arosa	9.68	46.78	1840	171
Zürich	8.56	47.38	556	170
Locarno-Monti	8.78	46.16	379	147

The downscaling methods are calibrated using the data from 1958–1978 and 1994–2000 and validated for the ERA-15 period 1979–1993. Seasonal values of all STARDEX indices were calculated for every year for the downscaled data. The present analysis is, however, restricted to the indices listed in Table 2.

Results

Mean annual cycle

The mean annual cycle for the indices AV, FRE, INT, and Q90 for the NCEP and downscaled data is shown in Fig. 2-5. The deviations from the observed annual cycle represent the bias of the data.

Table 2: STARDEX Diagnostic Extreme Indices considered in the present analysis.

name	description
AV	mean precipitation
FRE	precipitation frequency
INT	precipitation intensity
Q90	90th percentile of rainday amounts
X3D	maximum 3-day total precipitation
XCWD	max no consecutive wet days
PDD	mean dry-day persistence
XCDD	max no consecutive dry days

Thus, with respect to the bias, the two standard methods (LOC and DYN) and also the intensity downscaling methods (LOCI and DYNI) perform very similarly. For AV all four methods have a similarly high skill. For the other three indices (FRE, INT, Q90), the intensity scaling methods perform significantly better than the standard methods. Larger differences between DYNI and LOCI are only found for Q90. For some stations (e.g. Locarno-Monti, Zürich, and Arosa) DYNI is closer to the observations than LOCI.

Interannual variations

The skill in reproducing the correct interannual variability is illustrated for four typical stations in the Taylor diagrams shown in Fig. 6-9. Note the large differences in the skill from one index to another, and from one season to another, but also from one station to another. Generally higher skills are obtained for AV, FRE, and PDD, while generally lower skills are found for INT and Q90. Of the four stations, Locarno-Monti shows the overall best performance, followed by Zürich and Nice, and finally Bologna. Notice that the main difference between the methods is not in the correlation skill, but in the magnitude of the interannual variations (e.g. standard devation ratio). For Locarno-Monti, for instance, the best results are obtained for DYNI. This method is closest to the correct interannual variability (variance) for most seasons and most indices.

Fig. 10 shows a a direct comparison of the dynamical intensity scaling method (DNYI) with the raw NCEP data. In winter the downscaled data shows higher correlations for all indices and most stations. For the other three seasons (not shown) the picture is less uniform. For some indices and stations the correlation skill of the downscaled data is higher, while for other indices and stations it is lower. As was already found with the Taylor diagrams, the main improvement of the downscaled data is its magnitude of interannual variability (Fig. 11-14. As can be seen, for most stations and most indices the standard deviation ratio is closer to one for the downscaled data than for the raw NCEP data. Some example time series for four stations for Q90 and X3D are shown in Fig. 15 and 16.

The mean skill obtained for the ten Alpine stations for the raw NCEP and downscaled data is summarized in Table 3.

Conclusion

It has been found, that the downscaling skill varies considerably from station to station, from season to season, and from index to index. These variation are often larger than the differences between the different downscaling methods. Overall the intensity scaling methods (LOCI and DYNI) achieve higher skills than the standard methods (LOC and DYN). For most stations and indices, the added value of performing a flow-dependent scaling (DYN and DYNI) is relatively small.

Table 3: Mean skill for the ten Alpine stations for the downscaled and ncep raw data.

model	Correlation				RMSE			
	wi	sp	su	au	wi	sp	su	au
				AV				
(NCEP)	0.57	0.47	0.37	0.71	1.00	1.26	1.60	1.82
(DYNI)	0.63	0.52	0.47	0.68	0.60	0.84	0.96	1.03
(DYN)	0.66	0.56	0.51	0.71	0.56	0.75	0.86	0.98
(LOCI)	0.57	0.47	0.31	0.67	0.70	1.03	1.24	1.16
(LOC)	0.57	0.49	0.35	0.69	0.66	0.92	1.07	1.10
				FRE				
(NCEP)	0.75	0.55	0.48	0.74	0.12	0.18	0.26	0.11
(DYNI)	0.79	0.53	0.39	0.71	0.05	0.07	0.08	0.06
(DYN)	0.79	0.58	0.52	0.75	0.11	0.19	0.23	0.15
(LOCI)	0.79	0.58	0.38	0.70	0.06	0.08	0.08	0.07
(LOC)	0.80	0.56	0.49	0.75	0.12	0.19	0.24	0.15
				INT				
(NCEP)	0.27	0.16	0.11	0.47	5.28	5.04	6.01	7.74
(DYNI)	0.44	0.21	0.12	0.45	2.70	2.03	3.37	3.35
(DYN)	0.46	0.18	0.24	0.49	4.03	4.12	5.71	5.38
(LOCI)	0.28	0.22	0.04	0.43	3.00	2.19	3.12	3.43
(LOC)	0.25	0.18	0.11	0.45	4.47	4.80	6.39	6.00
				Q90				
(NCEP)	0.22	0.23	0.16	0.29	15.77	14.11	18.85	22.25
(DYNI)	0.38	0.19	0.25	0.35	10.28	7.96	12.19	12.24
(DYN)	0.35	0.20	0.25	0.38	12.74	11.81	17.45	16.06
(LOCI)	0.24	0.22	0.16	0.26	10.91	8.90	14.61	13.02
(LOC)	0.19	0.20	0.17	0.31	13.85	13.63	19.52	17.94
				X3D				
(NCEP)	0.33	0.29	0.32	0.41	38.38	38.75	48.42	63.84
(DYNI)	0.42	0.31	0.33	0.41	25.89	25.74	35.12	42.94
(DYN)	0.44	0.33	0.37	0.41	27.38	29.04	40.62	45.01
(LOCI)	0.31	0.29	0.28	0.35	29.61	30.98	43.76	46.74
(LOC)	0.31	0.25	0.27	0.30	32.22	36.41	49.77	51.73
				PDD				
(NCEP)	0.62	0.40	0.28	0.69	0.08	0.10	0.13	0.07
(DYNI)	0.66	0.42	0.41	0.70	0.05	0.08	0.07	0.05
(DYN)	0.69	0.42	0.39	0.71	0.07	0.09	0.11	0.08
(LOCI)	0.65	0.44	0.42	0.68	0.05	0.08	0.08	0.06
(LOC)	0.67	0.37	0.35	0.70	0.08	0.10	0.12	0.08
				XCWD				
(NCEP)	0.27	0.21	0.41	0.45	3.41	7.43	10.00	3.01
(DYNI)	0.39	0.15	0.18	0.39	2.14	3.44	3.13	1.92
(DYN)	0.35	0.10	0.42	0.40	3.61	7.81	9.02	4.01
(LOCI)	0.33	0.26	0.20	0.39	2.30	2.48	2.74	1.84
(LOC)	0.34	0.16	0.41	0.37	3.78	7.13	9.00	3.89
				XCDD				
(NCEP)	0.67	0.35	0.21	0.61	11.13	6.55	9.63	8.08
(DYNI)	0.72	0.36	0.14	0.65	9.34	6.66	10.57	7.39
(DYN)	0.66	0.36	0.18	0.62	10.39	6.67	9.02	7.96
(LOCI)	0.72	0.25	0.13	0.60	9.48	7.20	11.96	8.31
(LOC)	0.67	0.35	0.17	0.63	10.91	6.63	9.27	7.89

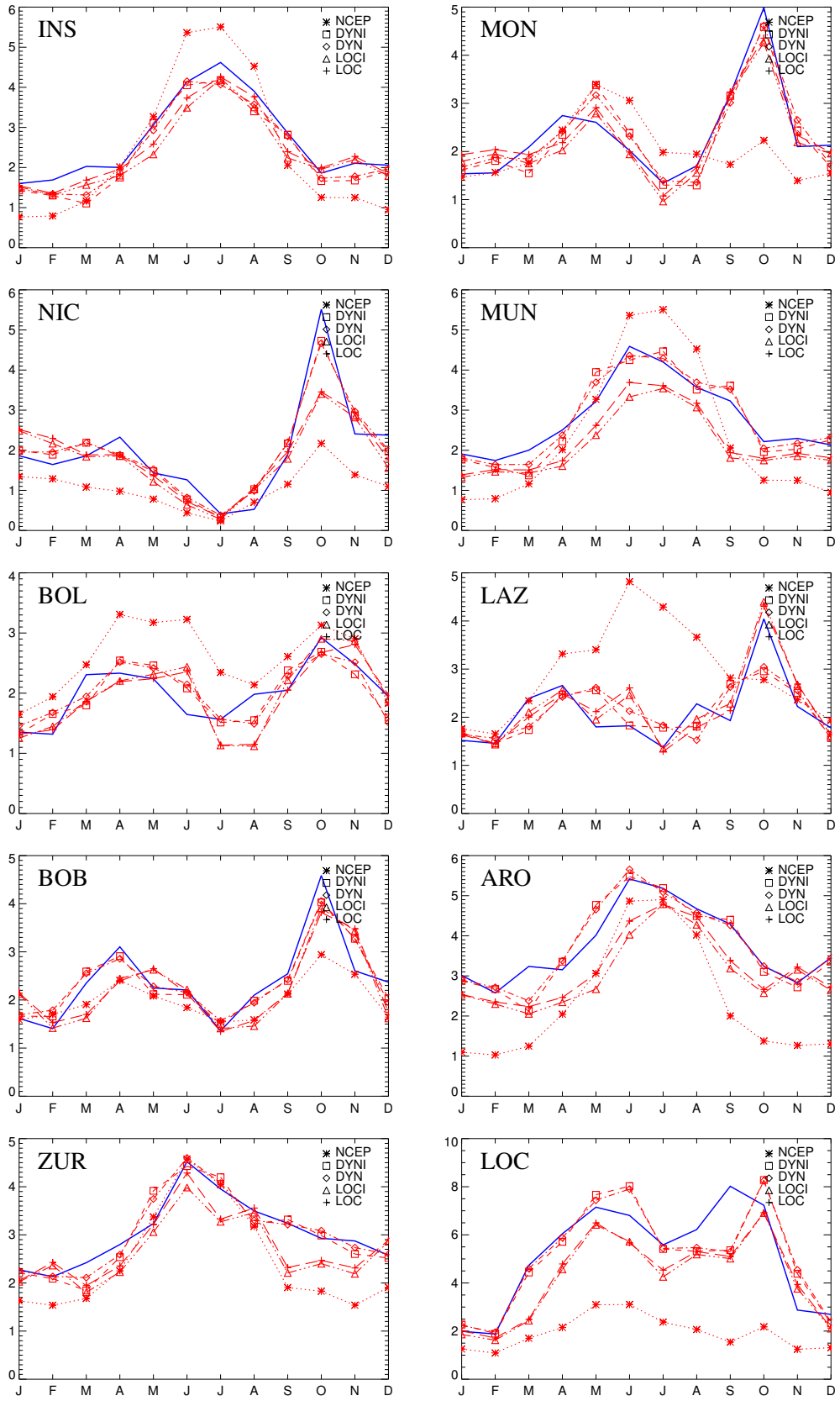

Figure 2: Mean annual cycle of AV for the ten Alpine stations deduced from observations (solid line), NCEP, and downscaled data.

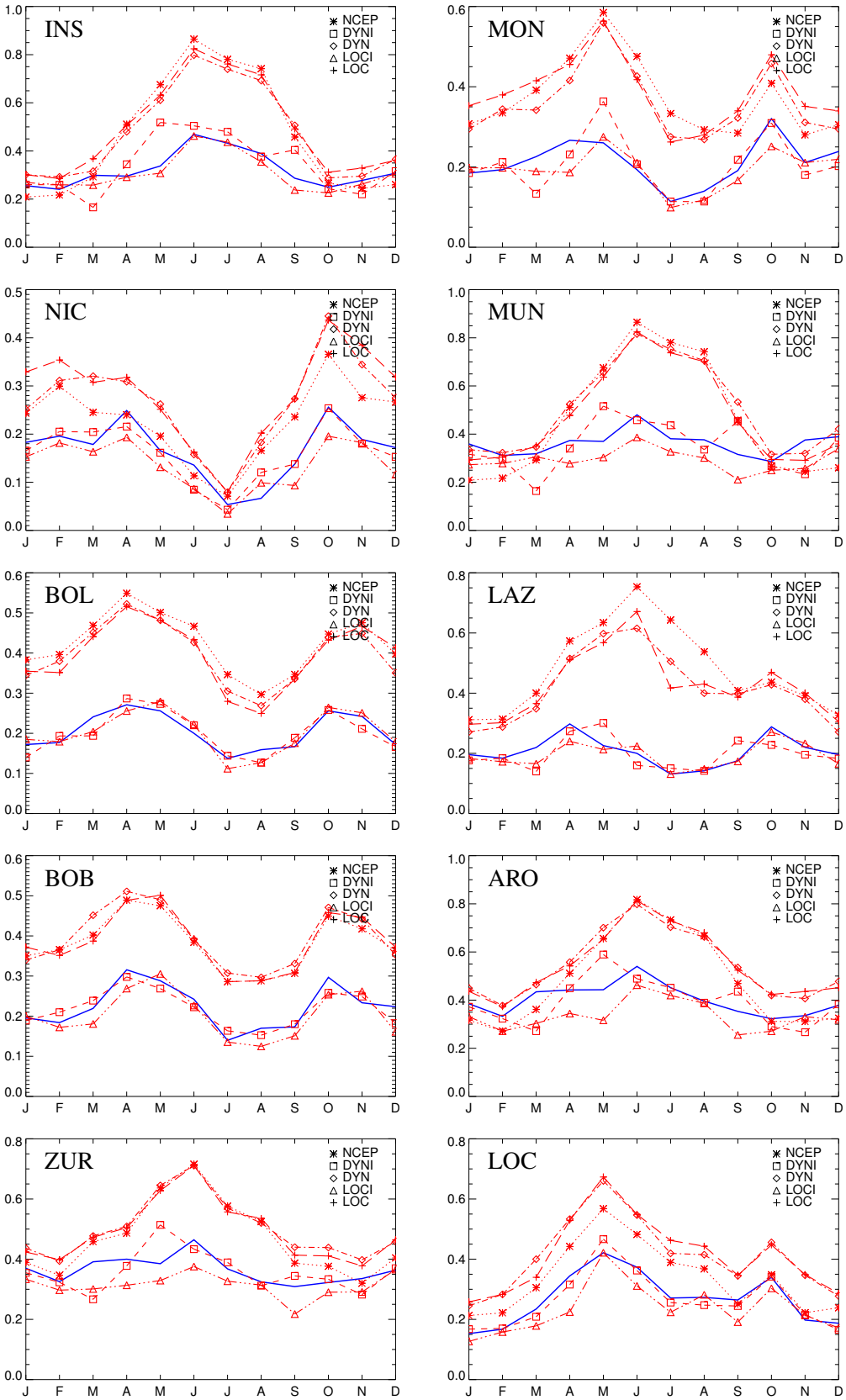

Figure 3: As Fig. 2, but for FRE.

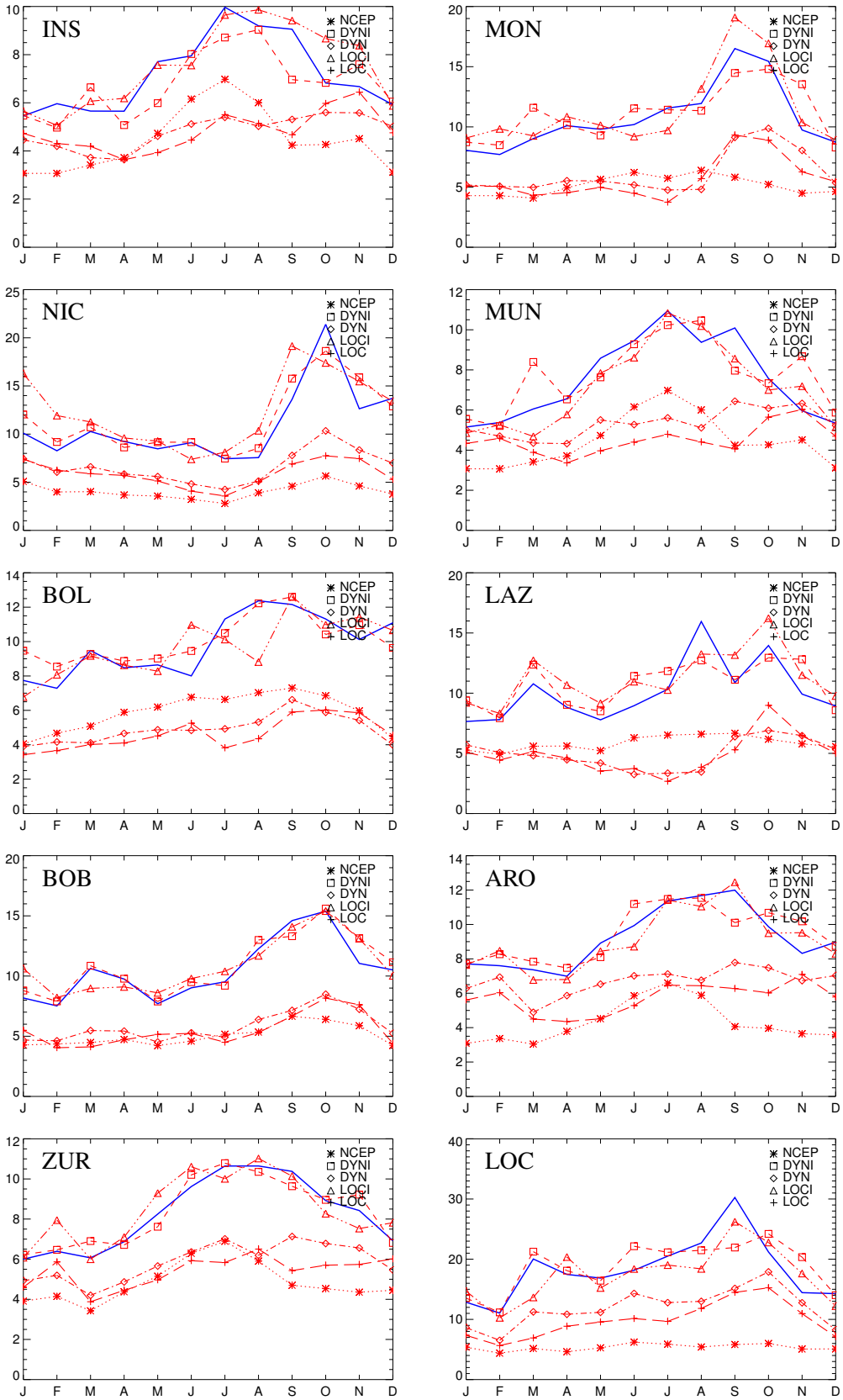

Figure 4: As Fig. 2, but for INT.

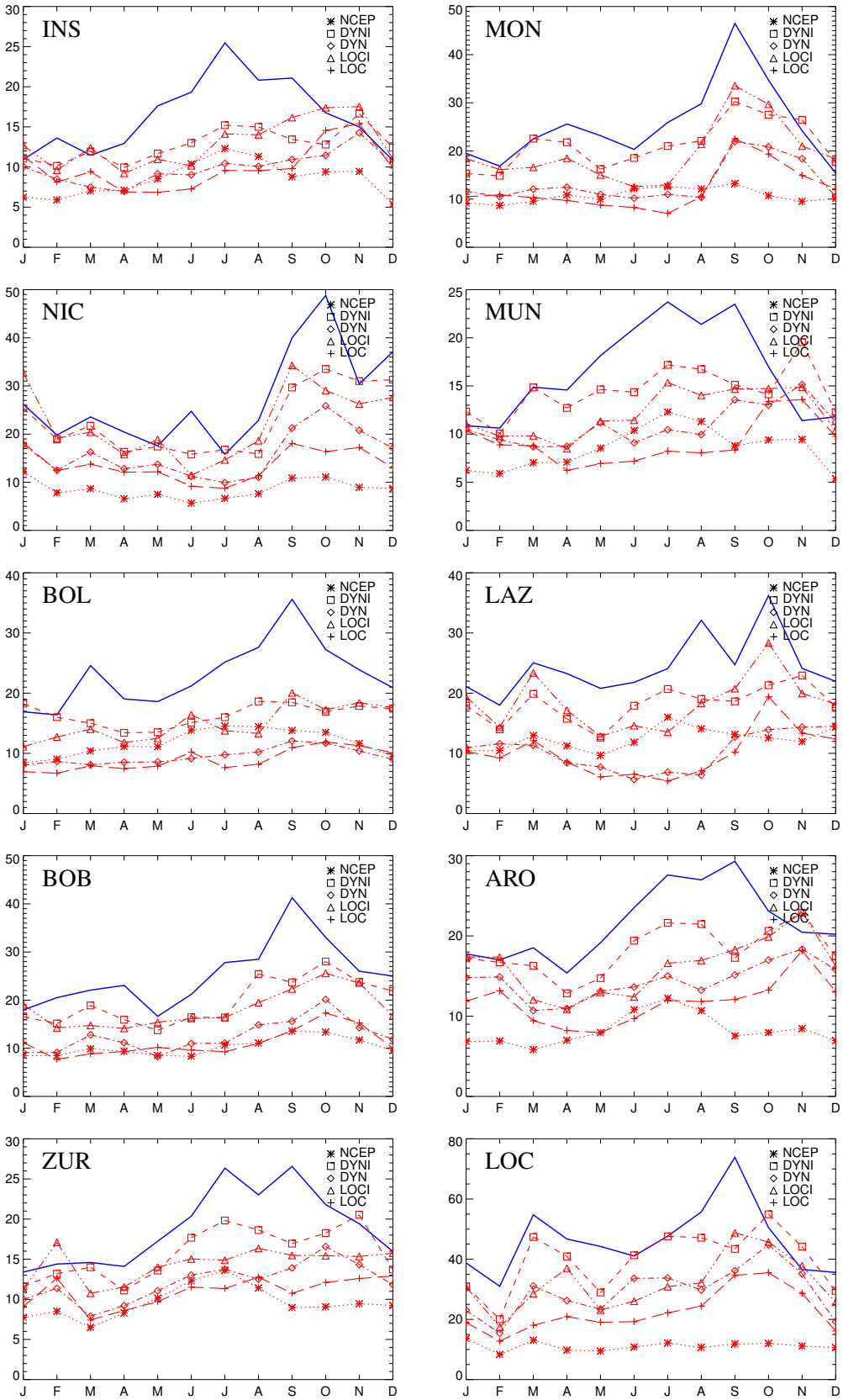

Figure 5: As Fig. 2, but for Q90.

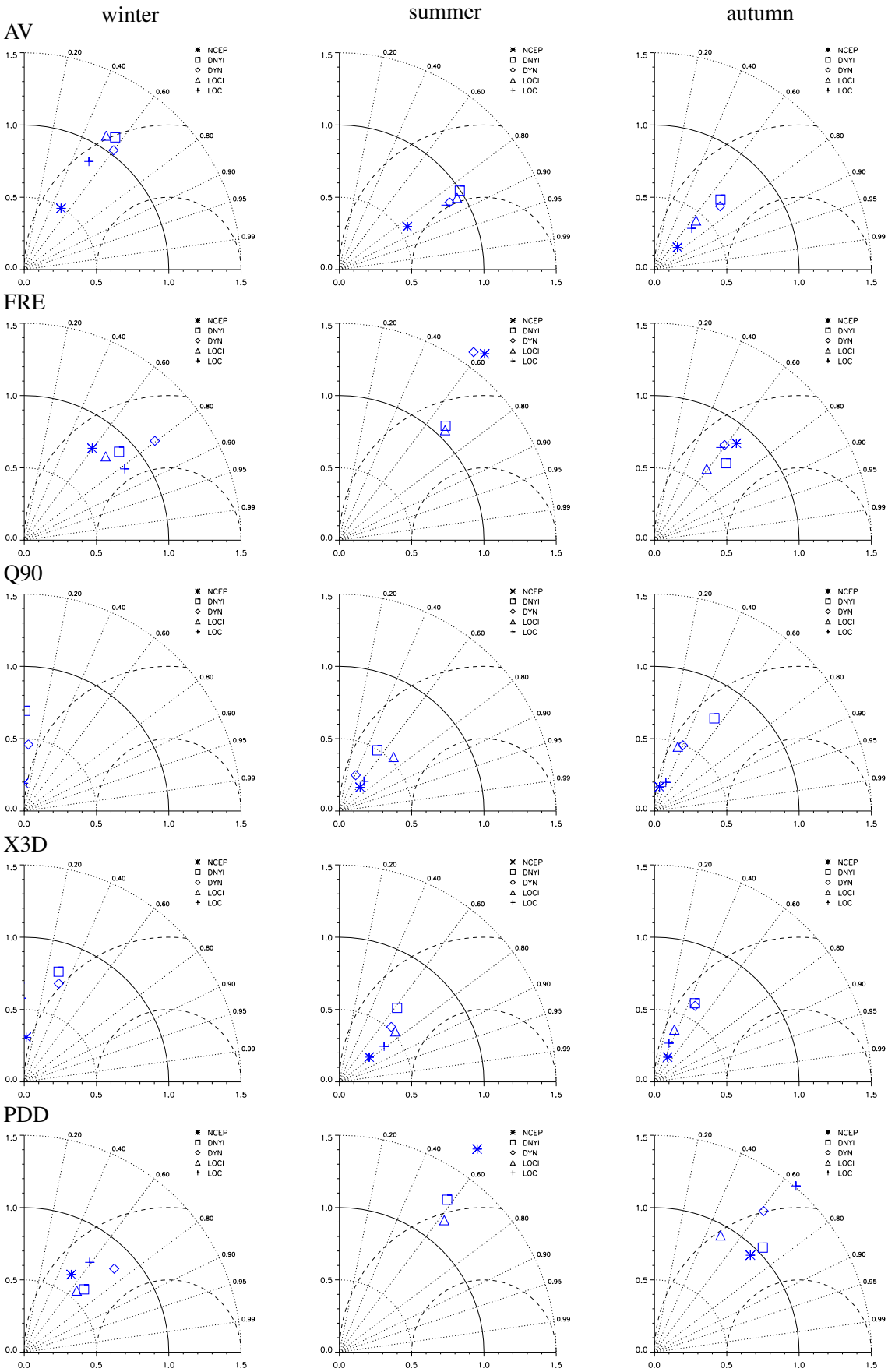

Figure 6: Taylor diagrams of interannual variability for Nice.

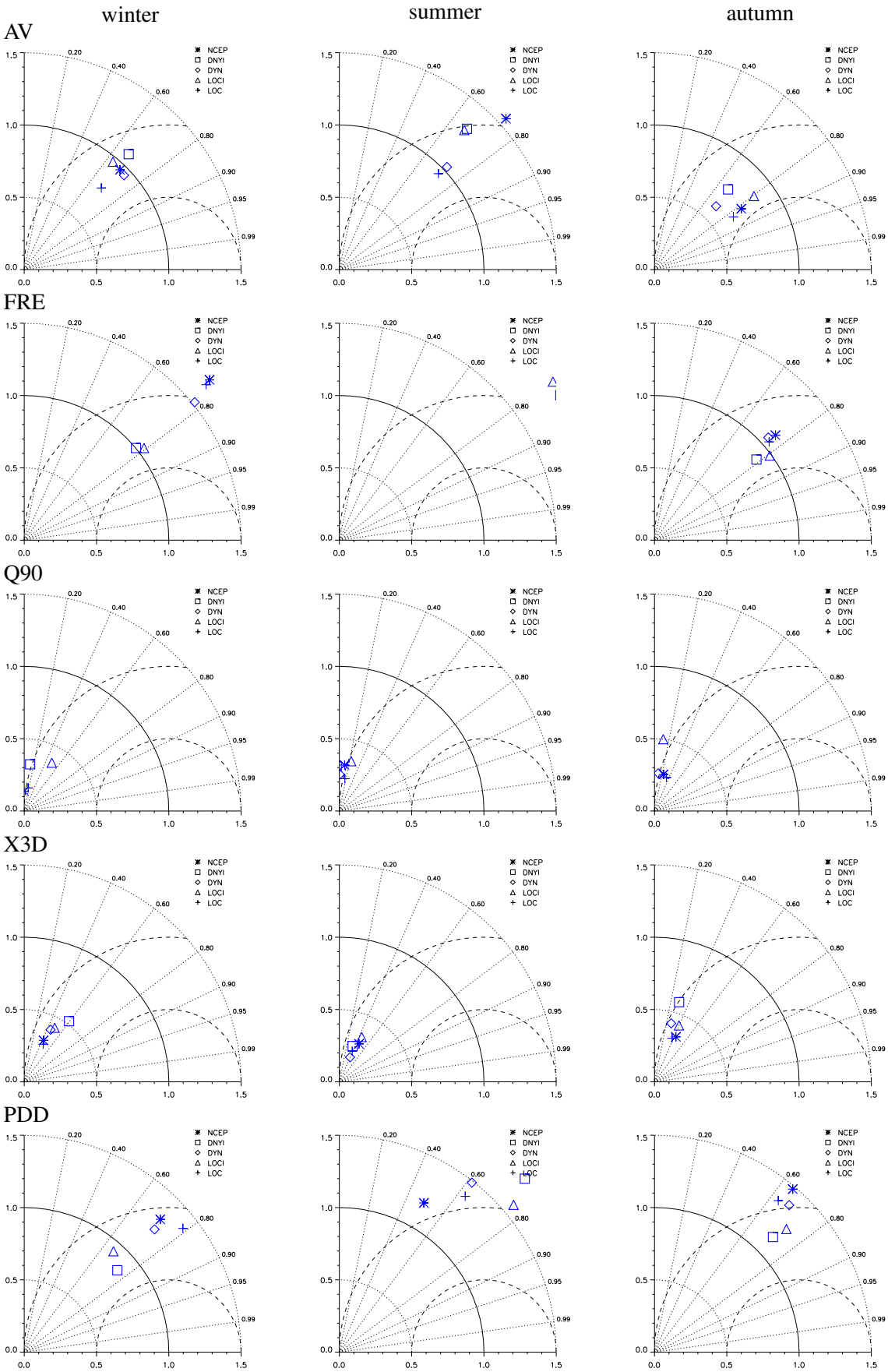

Figure 7: Taylor diagrams of interannual variability for Bologna.

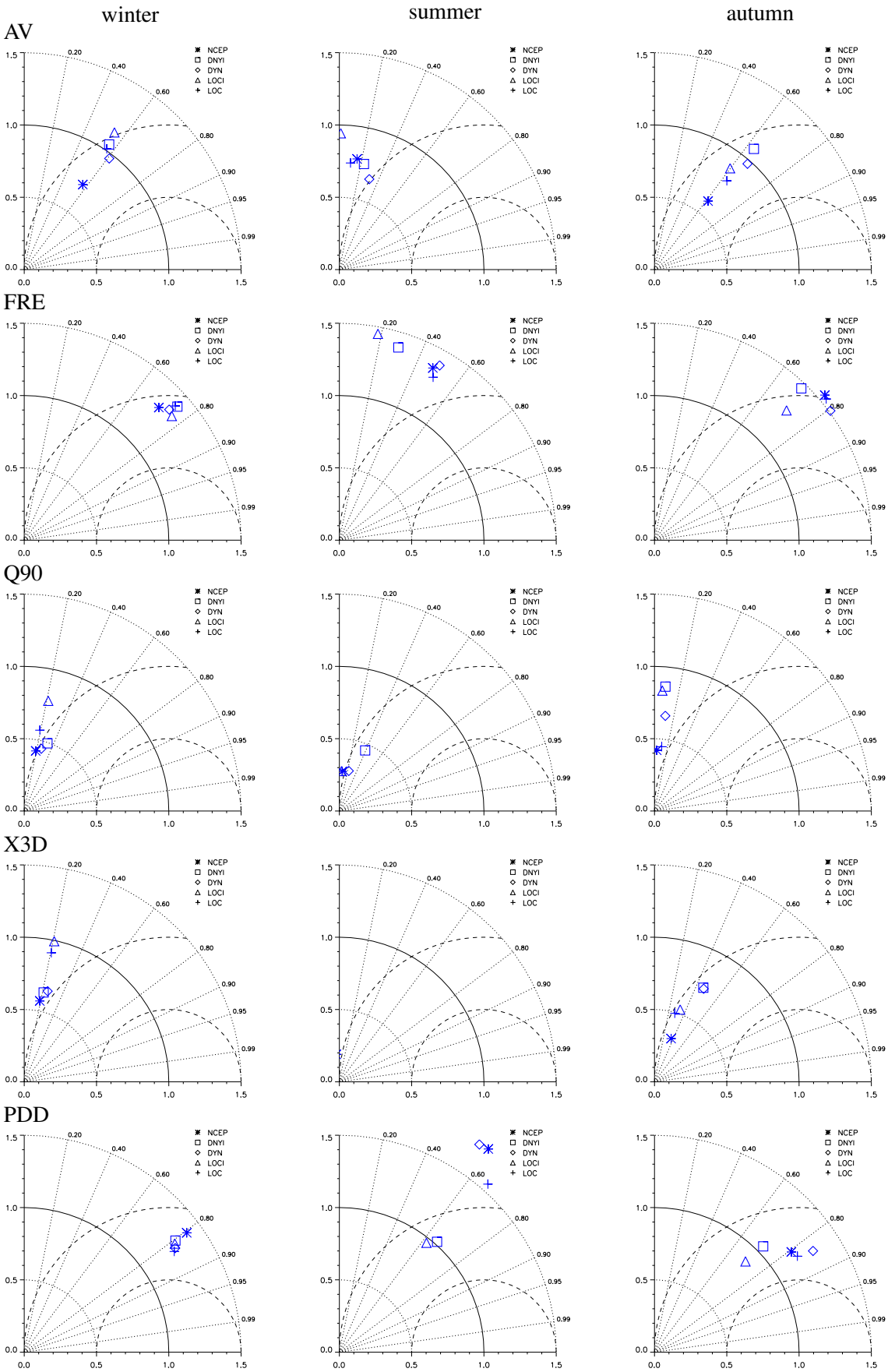

Figure 8: Taylor diagrams of interannual variability for Zürich.

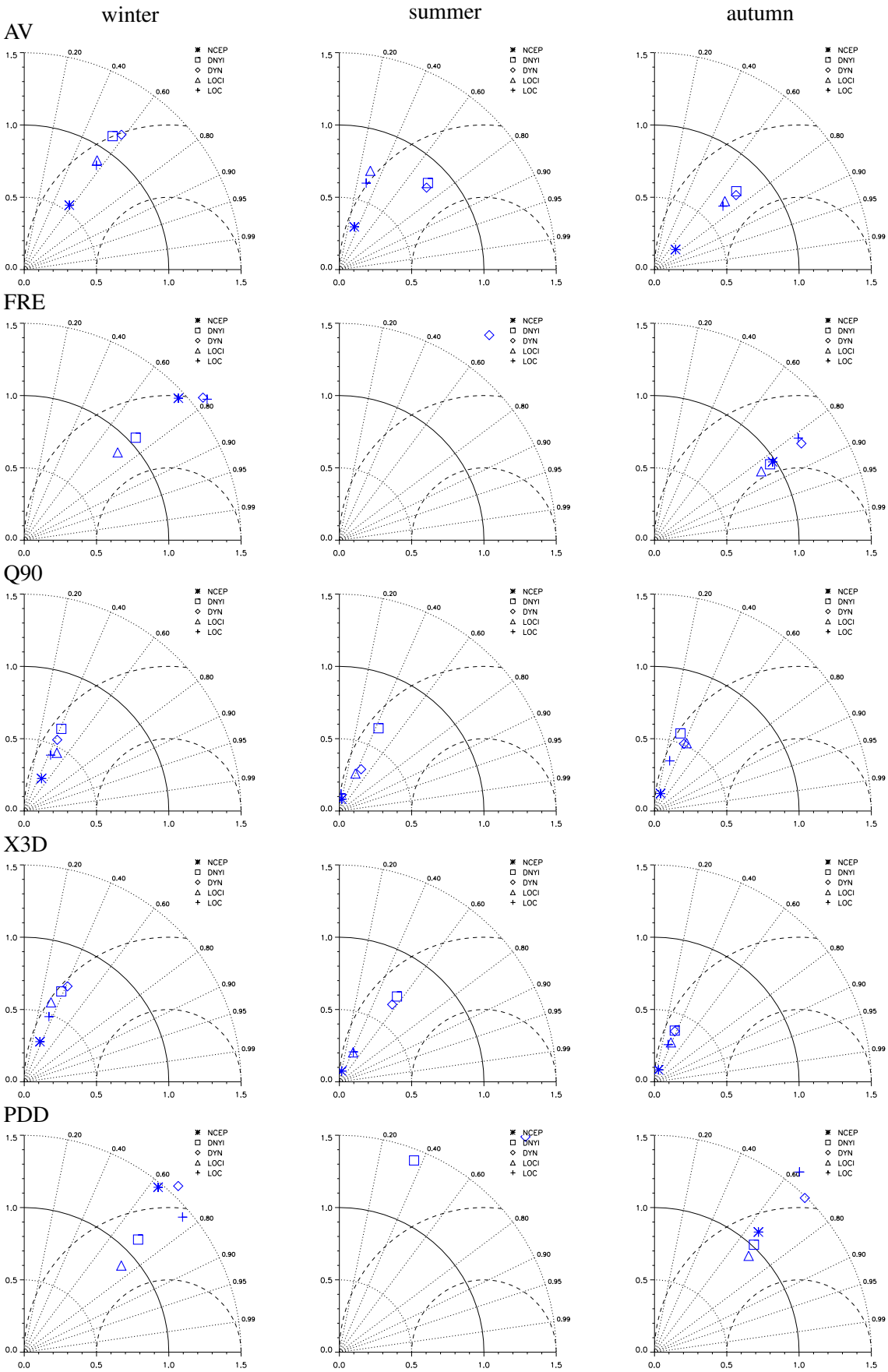

Figure 9: Taylor diagrams of interannual variability for Locarno-Monti.

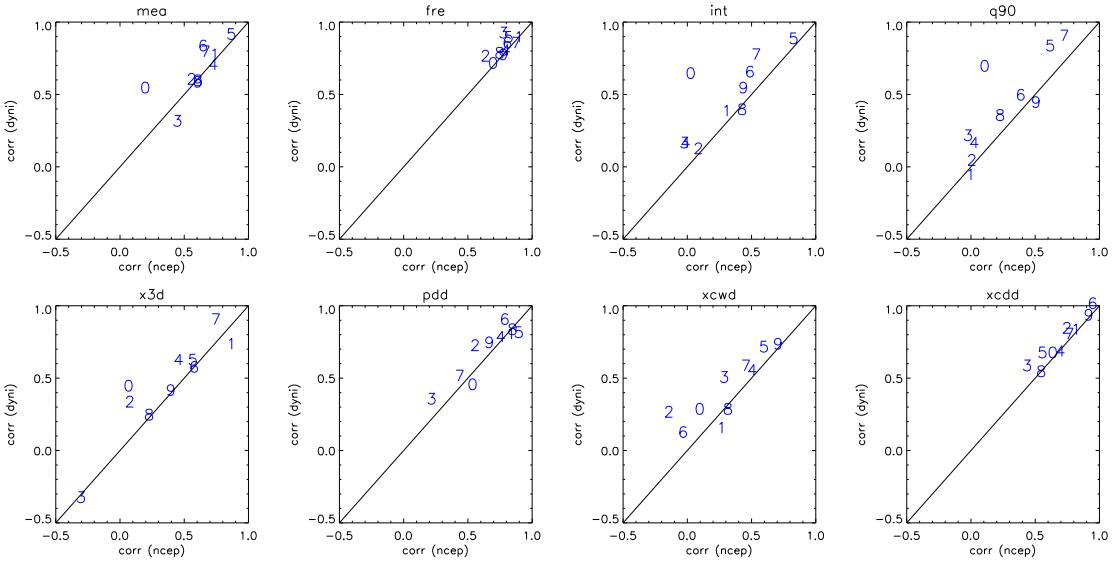

Figure 10: Correlation skill of dynamical intensity rescaling (DNYI) versus raw NCEP reanalysis for the winter season.

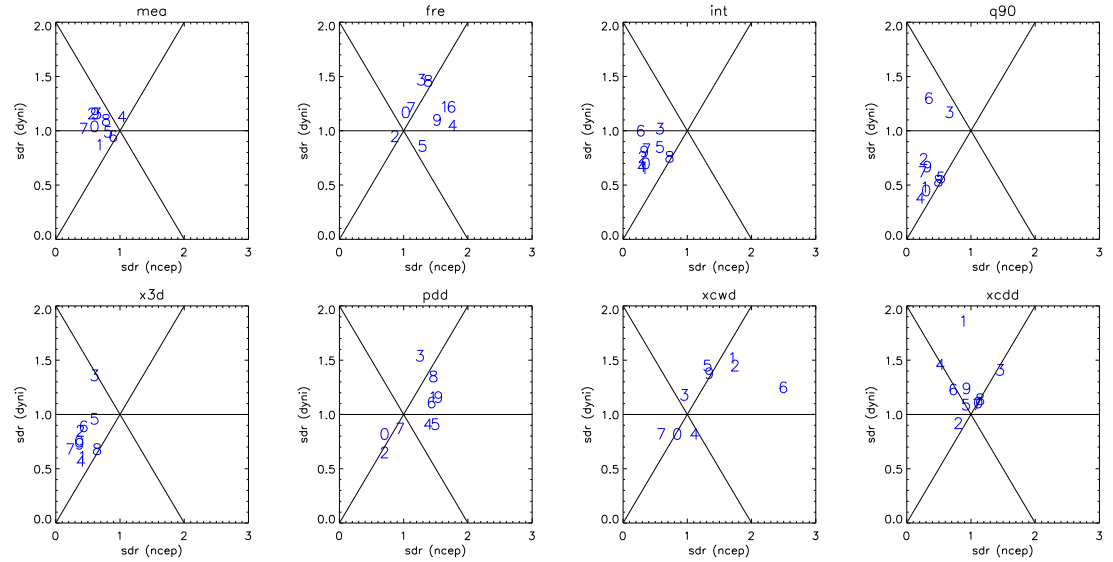

Figure 11: Standard deviation ratio skill of dynamical local rescaling versus raw NCEP reanalysis for the winter season.

References

Widmann, M. L., and C. S. Bretherton, 2003: Statistical precipitation downscaling over the Northwestern United States using numerically simulated precipitation as a predictor. *J. Climate*, **16**, 799–816.

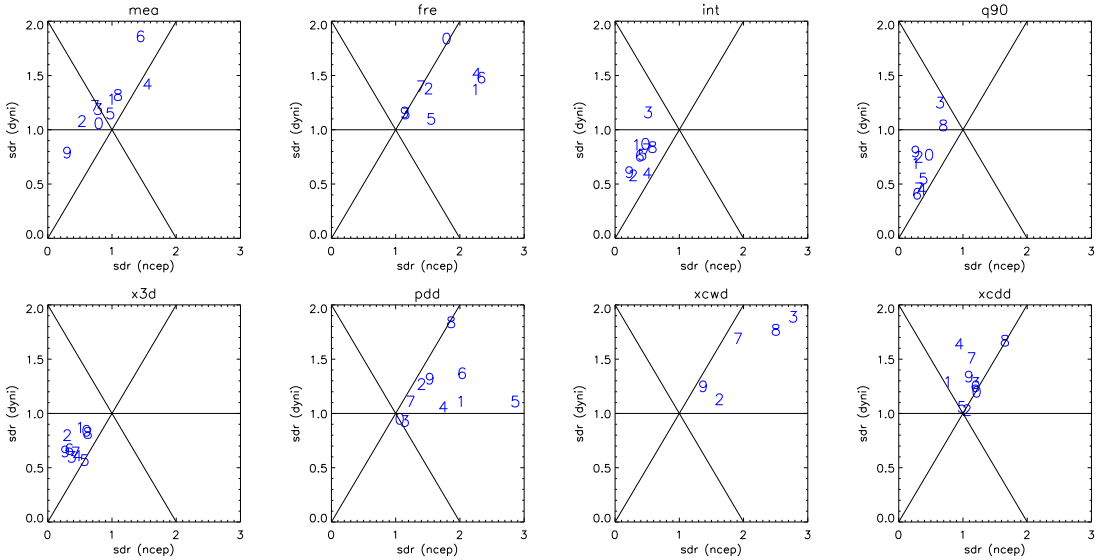

Figure 12: As in Fig. 11, but for spring.

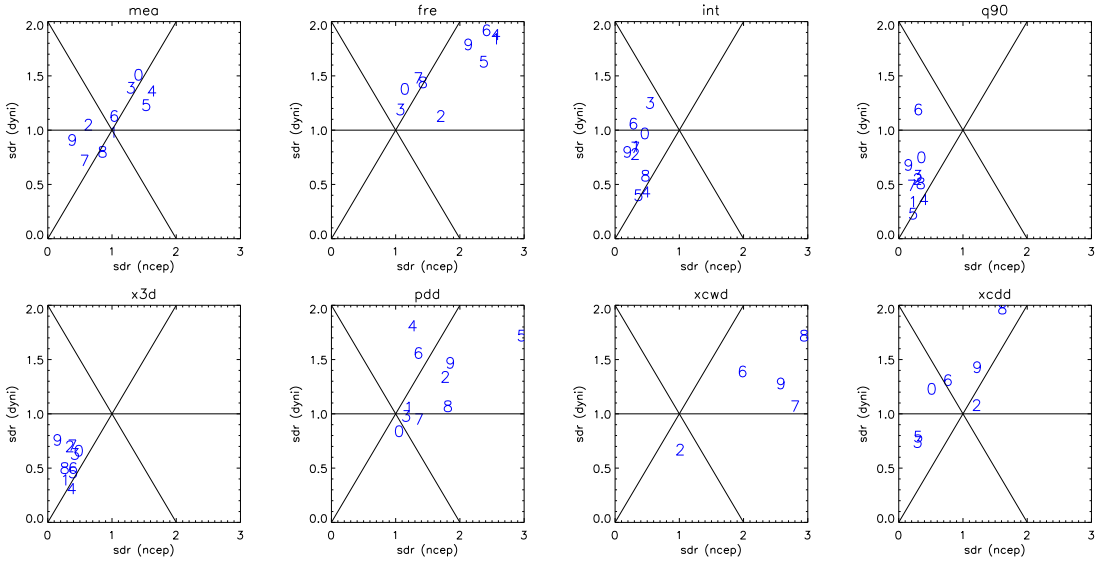

Figure 13: As in Fig. 11, but for summer.

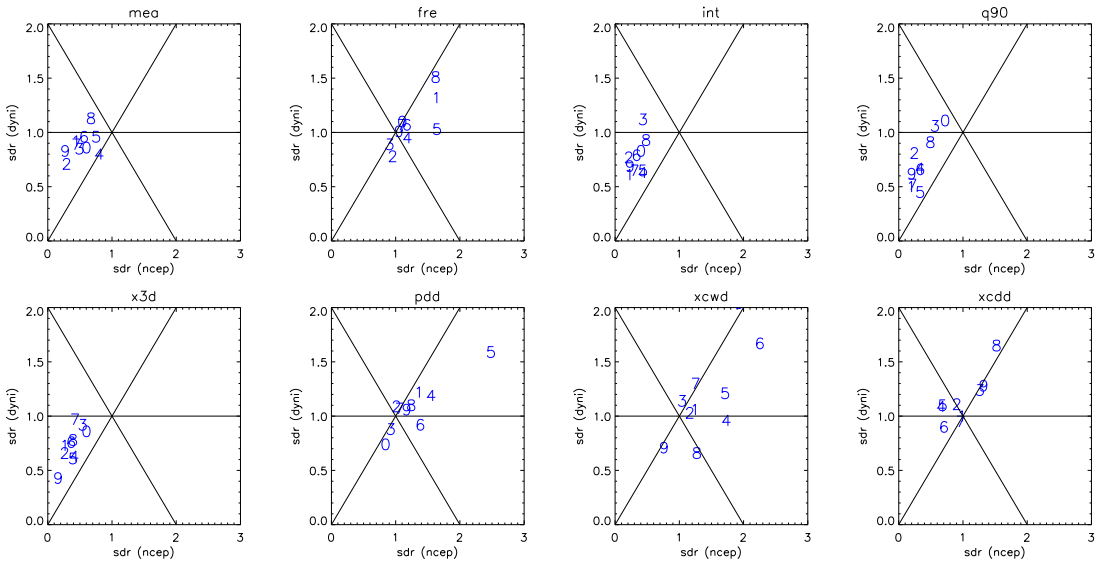

Figure 14: As in Fig. 11, but for autumn.

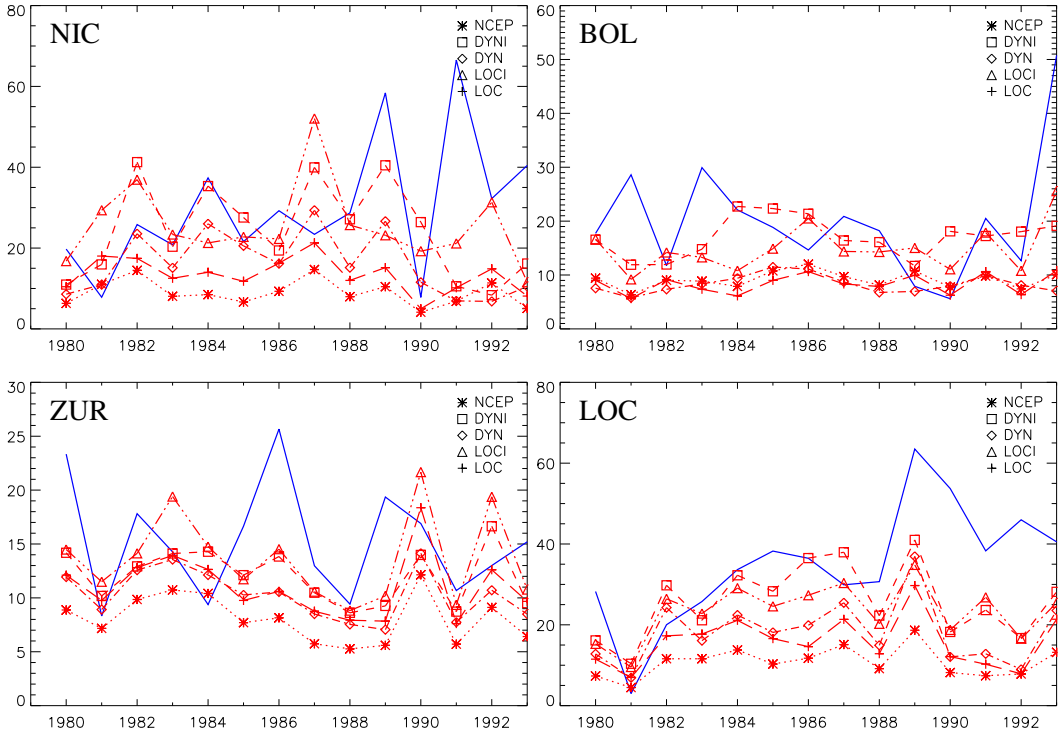

Figure 15: Time series of Q90 for four typical stations in winter.

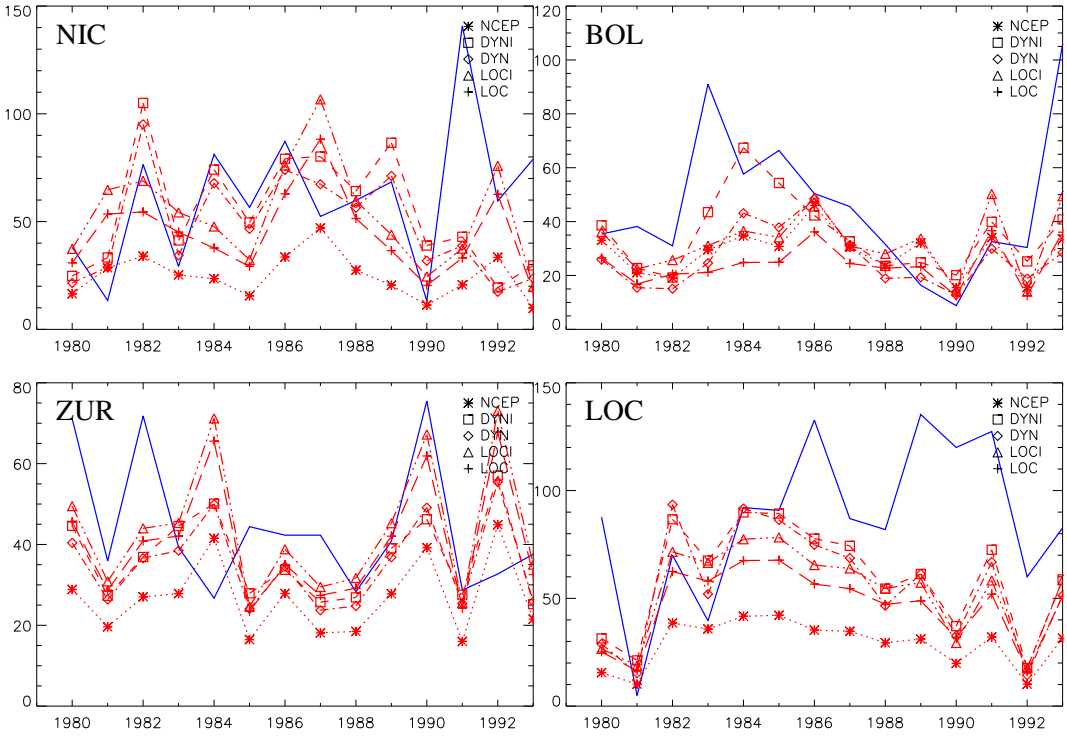

Figure 16: Time series of X3D for four typical stations in winter.